Comput Econ (2015) 46:243–273
DOI 10.1007/s10614-014-9457-4

Investigating the Performance of Non-Gaussian Stochastic Intensity Models in the Calibration of Credit Default Swap Spreads

Michele Leonardo Bianchi · Frank J. Fabozzi

Accepted: 18 July 2014 / Published online: 7 August 2014
© Springer Science+Business Media New York 2014

Abstract Most important financial models assume randomness is explained through a normal random variable because, in general, use of alternative models is obstructed by the difficulty of calibrating and simulating them. Here we empirically study credit default swap pricing models under a reduced-form framework assuming different dynamics for the default intensity process. We explore pricing performance and parameter stability during the highly volatile period from June 30, 2008 to December 31, 2010 for different classes of processes driven by Brownian motion, three non-Gaussian Lévy processes, and a Sato process. The models are analyzed from both a static and dynamic perspective.

Keywords Credit default swap · Cox-Ingersoll-Ross model · Non-Gaussian Ornstein-Uhlenbeck processes · Lévy processes · Sato processes · Filtering methods

Mathematics Subject Classification 60E07 · 60G18 · 60G51 · 91G40

1 Introduction

The mathematical setting needed for the pricing of credit derivatives can be viewed as a slight modification of models employed to price equity and interest rate derivatives. Most of the approaches proposed to improve standard pricing models for equity and interest rate derivatives have also been extended to obtain more reliable

M. L. Bianchi
Regulation and Macroprudential Analysis Directorate, Bank of Italy, Rome, Italy
e-mail: micheleleonardo.bianchi@bancaditalia.it

F. J. Fabozzi (✉)
EDHEC Business School, Nice, France
e-mail: frank.fabozzi@edhec.com

credit derivative pricing engines. In particular, certain arguments widely discussed in the literature—the analysis of risk premia, change of measure problem, affine processes, jumps in the underlying, and a suitable dependence structure for multivariate modelling—have been dealt with in the context of credit derivatives.

The fair value of complex financial derivatives, such as exotic options or baskets of credit default swaps, can be computed in two steps: (1) calibration of the parameters to the prices of liquid instruments traded in an active market; and (2) use of the parameters derived from the calibration exercise in step 1 to price more complex derivatives. This procedure implies that the fair value depends on the model's assumptions in both the calibration exercise and the evaluation part. As a result, the use of different models can lead to different fair valuations. For this reason, the first property that a model must have is the ability to explain the prices of liquid financial instruments traded on active and regulated markets in order to ensure a proper risk assessment and to limit possible arbitrage opportunities in more complex derivatives. Moreover, a model must be flexible enough to explain stylized facts observed in financial markets while at the same time possessing a satisfactory degree of computational tractability (see Cont 2001).

We discuss and empirically assess in this paper the performance of some pricing models to evaluate the prices of CDSs observed in the market. More precisely, we first extract risk-neutral parameters from the term structure of CDS spreads for more than 100 companies included in the Markit iTraxx Europe Index by considering five different models and then compare their pricing errors in the period from June 30, 2008 to December 31, 2010. Starting from three different classes of stochastic processes we analyze *reduced-form* or *intensity-based* models by assuming five different distributional hypotheses.

The underlying assumption made in most models is that the uncertainty in the financial markets can be explained through a normal distribution. However, there is considerable empirical evidence that the normal distribution is not flexible enough to explain the dynamics of complex financial products. The drawbacks of the normal model are by no means recent. The first attack came in the 1960s from Mandelbrot (1963) who strongly rejected normality as a distributional model for asset returns based on his study of commodity returns and interest rates. For this reason, particularly in the last decade, market participants have started applying more complex mathematical tools to finance in order to deal with possible mispricing caused by the use of normal-based models. The introduction of jumps and heavy-tails in the dynamics of stock returns (see Rachev and Mittnik 2000; Schoutens 2003; Cont and Tankov 2004, and Rachev et al. 2011) has been followed by the introduction of jumps in default modelling. Jumps in credit risk models can be introduced in two ways: (1) they can be included in the dynamics of the firm value process or (2) they can be included in the dynamics of the intensity process (see Schoutens and Cariboni 2009). In this paper, we focus on this second approach. Note that there is also the possibility of assuming a stochastic interest rate and adding jumps in both the instantaneous interest rate process and the default intensity process.

In the empirical analysis we investigate the classical Cox, Ingersoll and Ross (CIR) process applied to the modelling of default probabilities as proposed by Duffie and Singleton (1999); we then study Ornstein-Uhlenbeck (OU) default intensity processes

completely driven by jumps, as proposed by Cariboni and Schoutens (2009). Finally, we analyze a different framework where the default probability is explained via a Sato process, as proposed by Kokholm and Nicolato (2010). We compare three different families of stochastic processes in our empirical study: (1) the Brownian motion driving the CIR process; (2) Ornstein-Uhlenbeck processes based on Lévy processes, that is, non-Gaussian processes with independent and homogeneous increments (gamma, inverse Gaussian and variance gamma); and (3) additive processes (Sato), that is processes with independent but non-necessary homogeneous increments (see Sato 1999). Recall that the Brownian motion is a special case of Lévy process. It can be demonstrated that it is the only Lévy process with a continuous path. Jumps are introduced in the default intensity dynamics because CDS spreads exhibit large fluctuations and therefore it is necessary to account for this heavy-tailed nature of the risk (see Cont 2010) characterized by rare events and irregular jumps.

We consider two methodologies to estimate the proposed models: (1) we fit the models to daily CDS spreads observed in the market and check both the models' capabilities and the parameter stability (which we refer to as *static estimation*); and (2) we extract the unobservable default intensity process using filtering methods (which we refer to as *dynamic estimation*). Regarding the stability of the parameters, the static analysis shows that the Sato-based model outperforms its competitors and the parameter stability can be improved by incorporating regularization techniques into the optimization procedure. For the CDS spreads that we analyze and for the time period that we investigate, for static estimation the variance gamma based model seems to be satisfactory in terms of calibration error compared with all other competitor models, and in terms of dynamic estimation perspective it explains CDS price behavior better than the CIR model. Thus, we empirically find that the skewness and fat-tail properties of the default intensity process are also important for the pricing of CDSs.

In addition to the classical CIR model, we analyze models that allow only for positive jumps and a model that allows for two-sided jumps. Cont and Kan (2011) observed that, in analyzing daily returns on CDS spreads, both left and right tails appear to be heavier than those implied by the normal distribution, and models which only allow upward jumps, such as affine-jump diffusion models (see Duffie and Garleanu 2001) and non-Gaussian Ornstein-Uhlenbeck models with positive jumps (Cariboni and Schoutens 2009) may not be sufficient to explain the two-sided heavy-tailed behavior of CDS spreads. We confirm that these empirical findings cannot be captured by following the static estimation approach, but only by considering a dynamic estimation that explores the time-series properties of CDS spreads.

The remainder of this paper is organized as follows. A brief review explaining the mathematical framework of intensity-based models is provided in Sect. 2 and the stochastic processes employed in the empirical analysis are described in Sect. 3. In Sect. 4 we describe the data used in the empirical study. The two estimation methodologies based on (1) calibration on a daily basis, and (2) filtering methods that make use of the entire sample over the observed period are explained in Sect. 5, followed by a presentation and discussion of our results. Section 6 concludes the paper.

2 Evaluating CDS Sreads

We consider a reduced-form approach to model the default probability, assuming that the default intensity is a stochastic process (see Duffie et al. 2003). There is a general consensus for assuming a stochastic intensity instead of a deterministic intensity to model uncertainty about the future dynamics of the credit risk of a given reference entity. A similar framework has been used to price interest rate derivatives. However, for credit derivatives one models the default intensity process while for interest rate derivatives one models the spot rate or the factors explaining the term structure. More specifically, in a reduced-form model one assumes that the time of default is determined by the first jump time of a Cox process N_t starting from zero and with a stochastic intensity rate λ_t, where $0 \leq t \leq T$. Under this setting the default time τ is defined as $\tau = \inf\{t > 0 | N_t > 0\} = \inf\{t > 0 | A_t > E_1\}$, where the process A_t is usually defined as an *integrated process*, i.e.

$$A_t = \int_0^t \lambda_s \, ds$$

where λ_t is often a stationary affine process and E_1 is an exponential random variable with mean equal to 1. It follows that the survival probability up to time t is equal to

$$P_{Surv}(\tau > t) = \mathbf{E}\left[\exp(-A_t)\right] = \phi_{A_t}(i), \tag{1}$$

where $\phi_{A_t}(u)$, with $u \in \mathbb{R}$, is the characteristic function relative to A_t and $i = \sqrt{-1}$. Recall that the characteristic function of a random variable X is defined as $\phi_X(u) = \mathbf{E}\left[\exp(iuX)\right]$, $u \in \mathbb{R}$. By assuming a model for the intensity process λ_t we can compute the corresponding survival probability. If one knows the characteristic function of the process A_t, it is straightforward to compute the expectation in Eq. (1).

Recently, Kokholm and Nicolato (2010) analyzed a reduced-form approach where the default time is defined by the direct modelling of the process A_t. In their paper, the default is driven by an increasing and additive process, that is a process A_t with independent but not necessarily stationary increments.

By following the computations provided in O'Kane and Turnbull (2003) and Schoutens and Cariboni (2009), given a model for survival probability, one can easily derive the fair value of a CDS expiring at time T,

$$c_T^{CDS} = \frac{(1-R)\sum_i^n D(0,t_i)(P_{Surv}(t_{i-1}) - P_{Surv}(t_i))}{\sum_i^n D(0,t_i)P_{Surv}(t_i)\Delta t_i + \frac{1}{2}\sum_i^n D(0,t_i)(P_{Surv}(t_{i-1}) - P_{Surv}(t_i))\Delta t_i}, \tag{2}$$

where R is the recovery rate (usually assumed equal to 40 %), $D(0,t)$ is the discount factor, $t_1, \ldots, t_n = T$ represent the dates of payment at the end of each period t_i until maturity T. Here we assume a deterministic discount factor. Chen et al. (2008, 2013) considered a stochastic interest rate; Dunbar (2008) proposed a framework with stochastic factors to model interest rate and liquidity.

3 Cox-Ingersoll-Ross, Ornstein-Uhlenbeck and Sato Reduced-Form Models

In this section we describe different models based on the short-rate process approach first defined in the interest rate context. However, there are two main differences between interest rate and credit derivatives. First, as observed by Cont (2010), unlike the interest rate swap, the payoff of a CDS has a binary nature, that is, while the mark-to-market value of a CDS position prior to default may be small, the actual exposure upon default may represent a large fraction of the notional. Second, as outlined by Brigo and El-Bachir (2010), while the interest rate derivatives market is one of the most active financial markets with a large number of caps/floors, swaptions and other derivatives, the single-name CDS market presents a very small number of traded derivatives and the calibration of any model with a large number of parameters (for example, Rebonato et al. 2010) becomes unfeasible. In view of these differences, we start with the classical CIR model and extend the short-rate approach by modifying the distributional assumption without significantly increasing the number of parameters.

3.1 The CIR Process

A well-known way to model the default intensity process is to assume the CIR dynamics by considering the following mean-reverting process

$$d\lambda_t = \kappa(\eta - \lambda_t)dt + \vartheta\sqrt{\lambda_t}dW_t, \tag{3}$$

with $\lambda_0 > 0, \kappa, \eta$ and ϑ positive parameters, and $2\kappa\eta > \vartheta^2$ in order to ensure that the origin is inaccessible, that is, the intensity process does not reach zero. Under the CIR assumption there exists a closed-form expression for the characteristic function of the integrated CIR process and the survival probability in Eq. (1) can be computed as follows

$$P^{CIR}_{Surv}(\tau > t) = \frac{\exp(\kappa^2\eta t/\vartheta^2)\exp(-2\lambda_0/(\kappa + \gamma\coth(\gamma t/2)))}{(\coth(\gamma t/2) + \kappa\sinh(\gamma t/2)/\gamma)^{2\kappa\eta/\vartheta^2}}, \tag{4}$$

where $\gamma = \sqrt{\kappa^2 + 2\vartheta^2}$ (see Cox et al. 1985 and Schoutens and Cariboni 2009, for the derivation of the formula).

3.2 Non-Gaussian Ornstein-Uhlenbeck Processes

The CIR model can be enhanced by adding jumps and by considering the so-called jump diffusion CIR (JCIR) model as described by Brigo and Mercurio (2006) and by Lando (2004). Alternatively, one can consider a pure jumps mean-reverting process of the Ornstein-Uhlenbeck family. Over the past decade non-Gaussian Ornstein-Uhlenbeck (OU) processes introduced by Barndorff-Nielsen and Shephard (2001) have been widely studied from both empirical and theoretical points of view and have been applied in finance. This family of processes, which can capture important distributional properties observed in market prices for financial instruments, offers a more

flexible structure with respect to Gaussian-based models. This flexibility, together with the possibility to explain certain stylized facts of financial time series and a suitable degree of computational tractability, have increased the number of applications to finance, particularly, to stochastic volatility and interest rate modelling.

As defined by Barndorff-Nielsen and Shephard (2001), an OU process λ_t is a solution of a stochastic differential equation of the form

$$d\lambda_t = -\theta\lambda_t dt + dz_{\theta t}. \tag{5}$$

The unusual timing θt is deliberately chosen so that the marginal distribution of λ_t is independent of the choice of θ (see Barndorff-Nielsen and Shephard 2001). If z_t is an increasing Lévy process with finite variation starting from 0 and if $\lambda_0 > 0$, it can be proved that the process λ_t is strictly positive and bounded from below by $\lambda_0 \exp(-\theta t)$. If λ_t is an OU process with marginal law D, then it is referred to as a D-OU process. This means that if one starts the process with an initial value sampled from the D distribution, at each future time t, λ_t is distributed as D. Given a marginal law for D, and assuming that the law D is *self-similar* (see Sato 1999, for the definition of self-similarity), one can compute the characteristic function of the process z_t (the so-called *background driving Lévy process* - BDLP) as shown in Bianchi et al. (2013). The definition can be extended to non-increasing processes, as introduced by Barndorff-Nielsen (1997) and which has been widely studied (see Rosiński and Sinclair 2010).

In the rest of this section we describe OU processes with only positive jumps based on the gamma and on the inverse Gaussian (IG) distributional assumption, as well as an enhancement allowing for both positive and negative jumps based on the variance-gamma distributional assumption.

3.2.1 Mean-Reverting Processes with Only Positive Jumps

In the following we consider two examples of OU processes: the Gamma-OU and the IG-OU. Both hypotheses are particularly convenient because the characteristic functions of both the integrated Gamma-OU and the integrated IG-OU process are known in closed-form. Furthermore, there exist efficient algorithms to draw random paths by assuming these dynamics (see Barndorff-Nielsen and Shephard 2001 and Zhang and Zhang 2008).

Without further analysis of the properties of these processes, we provide the necessary formulas to evaluate the survival probability under these distributional assumptions (see Schoutens and Cariboni 2009 for the derivation of the formula). For the Gamma-OU case, by assuming a $\Gamma(a, b)$ process it can be proved that

$$P_{Surv}^{Gamma-OU}(\tau > t) = \exp\left(-\frac{\lambda_0}{\theta}(1 - \exp(-\theta t)) - \frac{\theta a}{1 + \theta b} \left(b \log\left(\frac{b}{b + \theta^{-1}(1 - \exp(-\theta t))} \right) + t \right) \right), \tag{6}$$

In the IG-OU case, by assuming a IG(a,b) process it can be proved that

$$P_{Surv}^{IG-OU}(\tau > t) = \exp\left(-\frac{\lambda_0}{\theta}(1-\exp(-\theta t) - \frac{2a}{b\theta}A(t)\right), \tag{7}$$

where

$$A(t) = \frac{1+\sqrt{1+\kappa(1-\exp(-\theta t))}}{\kappa} + \frac{1}{\sqrt{1+\kappa}}\left(\operatorname{arctanh}\left(\frac{\sqrt{1+\kappa(1-\exp(-\theta t))}}{\sqrt{1+\kappa}}\right) - \operatorname{arctanh}\left(\frac{1}{\sqrt{1+\kappa}}\right)\right),$$

with $\kappa = \frac{2}{b^2\theta}$.

3.2.2 Mean-Reverting Processes with Two-Sided Jumps

In this section we describe the variance-gamma Ornstein-Uhlenbeck process in the context of default modelling. As will be discussed in Sect. 5.2, under a state-space framework the use of a OU mean-reverting process with only positive jumps is not sufficient to obtain a satisfactory calibration error in the pricing of observed CDS spreads. To obtain greater flexibility in the calibration exercise we introduce a two-sided jumps Lévy-based OU model. This mean-reverting process belongs to the class of tempered stable as well as of hyperbolic Ornstein-Uhlenbeck processes (see Bibby and Sørensen 2003). This process can be viewed as the two-sided extension of the Gamma-OU process and also in this case Eq. (1) can be written in closed-form. Let C, λ_+, λ_- be positive constants, the law X is said to have a variance-gamma (VG) distribution if the characteristic function of X is given by

$$\phi_X(u) = E[\exp(iuX)] = \left(\frac{\lambda_+\lambda_-}{\lambda_+\lambda_- + (\lambda_+ - \lambda_-)iu + u^2}\right)^C. \tag{8}$$

The VG distribution can be viewed as the difference between two independent gamma distributions $\Gamma(C, \lambda_+)$ and $\Gamma(C, \lambda_-)$. Given a VG distribution, one can define the corresponding VG-OU process by assuming VG(C, λ_+, λ_-) and, as shown in Bianchi et al. (2013), it can be proved that

$$P_{Surv}^{VG-OU}(\tau > t) = \exp\left(-\frac{\lambda_0}{\theta}(1-\exp(-\theta t)) - \frac{\theta C}{1+\theta\lambda_+}\left(\lambda_+ \log\left(\frac{\lambda_+}{|\lambda_+ + \theta^{-1}(1-\exp(-\theta t))|}\right) + t\right) + \frac{\theta C}{1-\theta\lambda_-}\left(\lambda_- \log\left(\frac{\lambda_-}{|\lambda_- - \theta^{-1}(1-\exp(-\theta t))|}\right) - t\right)\right). \tag{9}$$

Even if the process may become negative, the asymmetric shape of the VG distribution and the additional assumption $\lambda_+ < \lambda_-$ make the VG-OU process proper

in many empirical applications. Furthermore, the inequalities $\lambda_+ < \lambda_-$ and $\lambda_0 > 0$ ensure that the survivor probability in Eq. (9) is well-defined. Finally, the Gamma-OU simulation algorithm can easily be extended to simulate VG-OU random variates.

3.3 The Sato Family

Sato processes can be viewed as an enhancement of Lévy processes as they have still independent but not necessarily stationary increments. This class of processes was introduced by Sato (1991), but it has been applied to finance only recently by Carr et al. (2007). As noted in Sects. 2, Kokholm and Nicolato (2010) analyzed a reduced-form approach where the default time is defined by the direct modelling of the process A_t. In Sect. 3.1 and 3.2 earlier in this paper, the increasing process A_t was modelled as the integral of a OU process. In this section, the process A_t is assumed to be increasing and additive, that is, a process with independent but not necessarily stationary increments. Here we review the construction of Sato processes, starting from the definition of self-similarity.

A process A_t is *self-similar* if

$$A_{\alpha t} = \alpha^{\gamma} A_t, \tag{10}$$

where the equality is in distribution and γ is named the self-similarity coefficient. Given a *self-decomposable* law (see Sato 1999, for further details). and a parameter γ, one can construct a self-similar process. By Eq. (10), the following equalities hold

$$\mathbf{E}\left[e^{iuA_t}\right] = \mathbf{E}\left[e^{iut^{\gamma}A_1}\right] = \phi_{A_1}(ut^{\gamma}). \tag{11}$$

If one knows the characteristic function of A_1, it is possible to have a closed-form expression for (11) and thus for (1). Furthermore, as observed by Kokholm and Nicolato (2010), the proposed model has a deterministic intensity process given by the equality

$$\lambda_t = \frac{d}{dt} \log \mathbf{E}\left[e^{-A_t}\right]. \tag{12}$$

Both the gamma and the IG random variable are self-decomposable, and the expectation in (11) has a closed-formula. If A_1 is a $\Gamma(a, b)$ random variable, A_t is referred to as a *Sato-Gamma* process, and if A_1 is a IG(a,b) random variable, A_t is called a *Sato-IG* process. As these processes are similar, we consider only the Sato-Gamma assumption in the empirical analysis. As shown in Kokholm and Nicolato (2010), in the Sato-Gamma model it can be demonstrated that

$$P_{Surv}^{Sato-Gamma}(\tau > t) = \frac{1}{(1 + t^{\gamma} b^{-1})^{a}}. \tag{13}$$

Table 1 Summary statistics of the CDS spreads between June 30, 2008 and December 31, 2010 for the 117 companies considered in the empirical study

	Years to maturity				
	1	3	5	7	10
Minimum	5.49	14.57	22.43	25.54	29.15
5th percentile	20.75	35.14	45.93	50.22	53.55
Mean	93.41	110.36	120.69	122.28	124.70
Median	56.44	78.89	92.93	96.05	100.13
95th percentile	283.51	290.06	283.40	274.41	267.78
Maximum	3257.54	3261.32	3127.44	2912.14	2800.06
Standard deviation	132.94	121.92	112.30	105.44	100.70
Mean absolute deviation	67.34	63.67	59.74	56.76	54.88
Median absolute deviation	27.48	30.47	31.46	30.49	30.26
Lag-5 autocorrelation	0.96	0.95	0.93	0.92	0.91

4 The Data

This section provides a description of the data used in the empirical analysis. We consider CDS spread data for 117 of the 125 companies included in the Markit iTraxx Europe Index (Series 12) from June 30, 2008 to December 31, 2010. The dataset includes the highly volatile period after Lehman Brothers filed for Chapter 11 bankruptcy protection (September 15, 2008).

Mid, bid and ask spreads for maturities 1, 3, 5, 7, and 10 years are obtained from Bloomberg. We are aware of the fact that (1) Bloomberg data does not necessarily refer to real transactions because it picks up market quotes (and not transaction prices) provided by its contributors, (2) the collected bid-ask difference could not reflect the real liquidity of the market, (3) the data can be different among data providers, as recently observed by Mayordomo et al. (2013), and, (4) the transactions generally involve the 5-year maturity contracts as described in Amadei et al. (2011). Eight companies have been discarded because their spreads are not available for the entire period. This is the reason that we analyze the default term structure for only 117 of the 125 component companies of the index. For each company and for each maturity, we have 655 observations, giving us a total of more than 380,000 CDS spreads. Table 1 provides summary statistics on the distribution of the companies analyzed in the sample period. In general, for all companies and for all maturities, CDS spreads increased sharply after Lehman's failure and bid-ask spreads widened, particularly for the shortest maturity. On September 17, 2008, Bloomberg reported that there was a flight to safety as investors sold off their positions in credit risky assets and invested those funds in short-term Treasury bills, resulting in Treasury bills rates falling to their lowest level since World War II. Moreover, the EURIBOR-OIS spread reached unexpected levels. Figure 1 shows the behavior of the mean and the median of CDS and bid-ask spreads in the period analyzed. Recall that the difference between the 3-month Euro interbank offered rate (EURIBOR) and the overnight indexed swap (OIS) is a measure of both credit and liquidity risk.

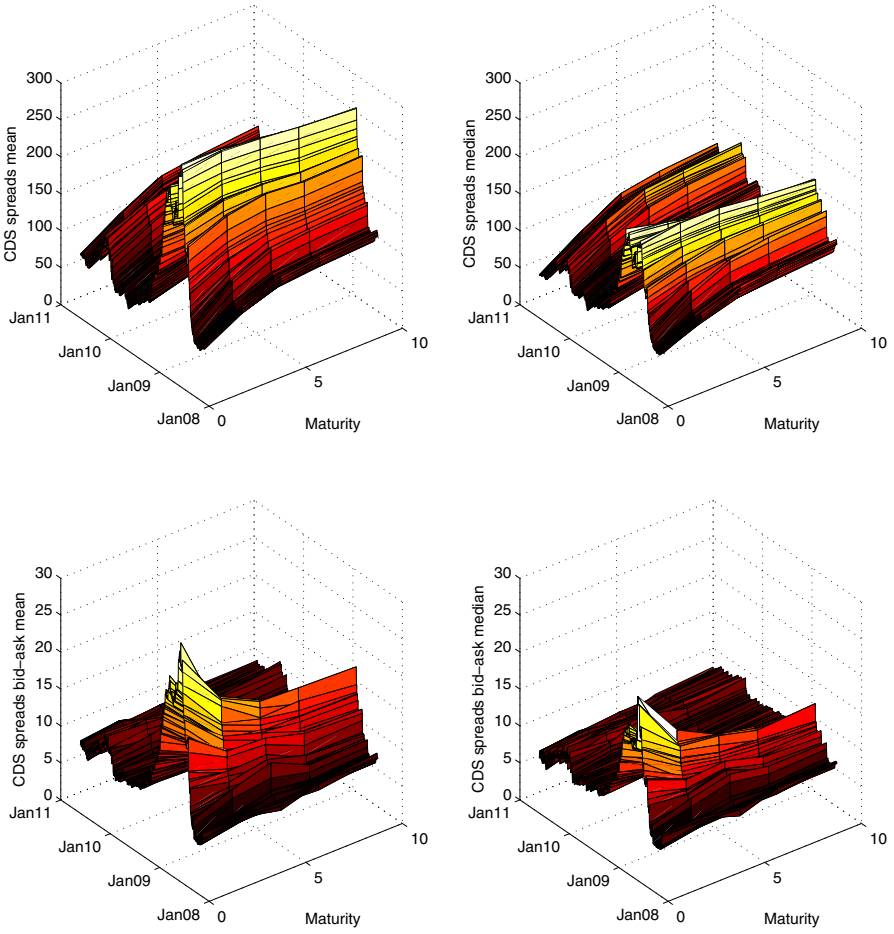

Fig. 1 Mean and median CDS and bid-ask spreads for the 117 companies considered in the empirical study

Pan and Singleton (2008) observed that the use of a stochastic interest rate model does not greatly modify the estimates; for this reason, we assume the risk-free term structure to be known. Risk-free rates are extracted from the LIBOR swap rate for short-term maturities up to 9 months and the EU swap curve for maturities from 1 year to 30 years (for a discussion on the choice of the *risk-free* rate, see Hull et al. 2004). At each given day and for each maturity the discount factor is computed by a linear interpolation of the risk-free term structure.

5 Empirical Results: Parameter Estimation

There are two possible methodologies to estimate a reduced-form model: (1) fit the model to the daily spreads observed in the market and check both the model

capabilities and the parameter stability; or (2) extract the unobservable default intensity process (or processes) by using a *filter* as described by Lando (2004) and empirically tested by Jarrow et al. (2011). The Kalman filter and its extensions can be taken into consideration when the intensity model is Gaussian, otherwise a *particle filter* framework has to be applied (see van der Merwe et al. 2001).

The first approach can be viewed as a short-term or static estimation for the purpose of pricing and hedging on a daily basis, and for this reason this approach is referred to as the *market maker approach*. Under this perspective, at each given point in time the model prices have to be as close as possible to the market prices and, even if the market is quoting unreasonable prices, market makers have to find the parameters that replicate those prices. The market maker needs to achieve static consistency in order to provide at each given point in time two-sided quotes. The goal is usually achieved by considering models with a large number of parameters.

The second approach is a long-term or dynamic estimation where the default intensity process is estimated by *filtering* the new information for the purpose of assessing the long-term default probability of the reference entity. Estimated model parameters can be used to make projections on price movements and trade the difference between the model prediction and the market quotes. These investment strategies (known as *statistical arbitrage strategies*) are commonly used by hedge funds and banks' proprietary trading desks and, for this reason, this second estimation methodology is referred to as the *long-term convergence trader approach*. Under this second perspective, one assumes that the model can beat the market or, more precisely, one trusts the model prices and tries to find possible arbitrage opportunities by looking at the differences between model and market prices. Dynamic consistency is important for long-term convergence trading, and pricing errors represent trading opportunities.

In this Section we apply both approaches. In Sect. 5.1 we analyze one-factor models based on five distributional assumptions, namely CIR, Gamma-OU, IG-OU, Sato-Gamma, and VG-OU based model. In Sect. 5.2 we cast the model into a state-space framework and by using filtering methods we calibrate one-factor models based on the CIR and VG-OU processes.

5.1 A Static Perspective: The Market Maker Approach

First, we investigate empirically the market maker approach in order to study the pricing performance on a daily basis and the parameter stability during a market downturn. From a practical perspective, on each trading day we minimize the root mean square error (RMSE) given by

$$RMSE(\Theta) = \sqrt{\sum_{T_i} \frac{(c_{T_i}^{CDS\ market} - c_{T_i}^{CDS\ model}(\Theta))^2}{\text{number of observations}}} \tag{14}$$

where T_i are the different maturities and Θ is the parameter vector according to a given model.

Since the minimization of Eq. (14) with respect to the parameter vector Θ has neither a closed-form solution nor a global minimum, a numerical optimization routine is needed to find a relative minimum. We use the Matlab r2008b function *fmincon*. The procedure was run on a Pentium D 3.00GHz with 2GB of Ram. As already observed by Fang et al. (2010), the minimization of Eq. (14) is a well-known ill-posed problem, mainly because the solution is not necessarily unique and there is no guarantee that a solution exists. For this reason we consider a regularization term of the form

$$f(\Theta) = \rho \|\omega \cdot (\Theta - \Theta_0)\|^2 \tag{15}$$

where ρ is a given constant parameter, Θ_0 is a given set of model parameters, ω is a vector selected to give the same weight to each parameter (see the Appendix), and "$\cdot$" denotes the inner product of vectors. The optimization problem becomes

$$\hat{\Theta} = \min_{\Theta} \left(RMSE(\Theta)^2 + \rho \|\omega \cdot (\Theta - \Theta_0)\|^2 \right). \tag{16}$$

Furthermore, this approach leads to more parameter stability over time. The choice of the parameter ρ influences the model calibration; however, ρ cannot be fixed in advance but depends on the data at hand and the level of error present in it (see Cont and Tankov 2004 and Fang et al. 2010). In the calibration exercise, we consider two values for ρ as follows. First, we solve the optimization problem (16) without regularization techniques, that is $\rho = 0$. Then we solve the optimization problem with $\rho = 100$. This last value for ρ shows a good balance between pricing performance and parameter stability (see the Appendix).

Then, we add some constraints to the problem in order to obtain more stable parameters over time and avoid the CIR and the VG-OU process hitting the zero bound. In the CIR case, we force the parameters $(\kappa, \eta, \vartheta, \lambda_0)$ in the region between (0.1, 0.005, 0.05, 1e-5) and (0.8, 0.05, 0.25, 2.5). In the one-sided jumps OU cases, we choose the following constraints for $(\theta, a, b, \lambda_0)$: for the Gamma-OU model (0.1, 0.1, 10, 1e-5) are the lower bounds and (4, 150, 40,000, 2.5) the upper ones, for the IG-OU model (0.25, 0.2, 10, 1e-5) are the lower bounds and (3, 2, 100, 2.5) the upper ones. In the Sato case, we fix $a = 0.5$ and (γ, b) can vary between (0.5, 5) and (5, 1,500). Finally, in the VG-OU case, (0.1, 0.1, 10, 10, 1e-5) are the lower bounds and (4, 150, 10,000, 10,000, 2.5) the upper ones of the parameters $(\theta, C, \lambda_+, \lambda_-, \lambda_0)$ and we add the inequality constraint $\lambda_+ < \lambda_-$, which in practice means that the positive tail is "fatter" than the negative one. Furthermore, in the non-regularized problem, the starting point of the optimization procedure is kept fixed and in the regularized problem the starting point of a given day is the optimal solution computed for the previous day.

We observe that in the one-sided jumps OU models, the calibration can be problematic as CDS spread values are mainly governed by the ratio a/b, but the parameters a and b are difficult to calibrate separately. By fixing as the starting point a large value for a (for example, $a = 100$), one obtains in the calibration procedure a large value for b as well ($b >> a$), therefore the variance of the intensity OU process becomes very small (in this case, the ratio $a/b = k$). By fixing as the starting point a smaller value for a' (for example, $a' = 2$) one obtains in the calibration procedure a smaller

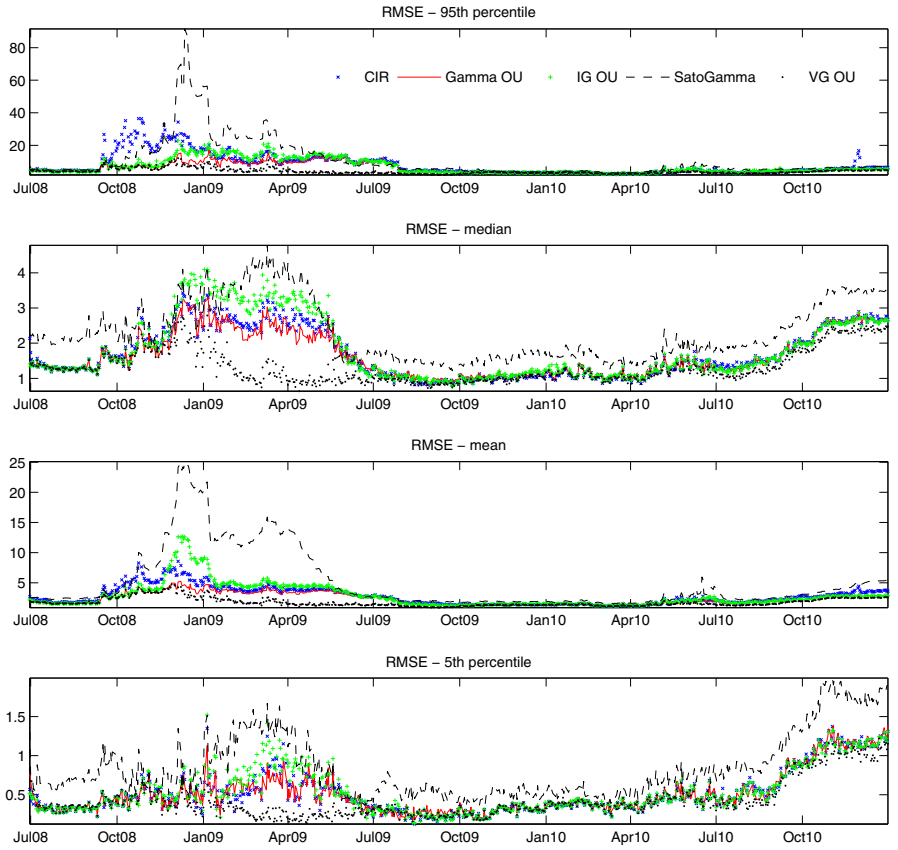

Fig. 2 Median, mean, 95th and 5th percentile of the RMSE for the 117 companies considered in the analysis. We report the pricing error obtained with $\rho = 100$

value for $b'(b' < b)$. At the same time the ratio $a'/b' = a/b = k$, the pricing error is quite close to the previous and the estimated variance is greater. In order to obtain a greater variance for the calibrated OU processes comparable with that of the CIR based model, we select as starting points in the Gamma-OU and in the IG-OU cases $a = 2$ and $a = 0.5$, respectively. Under this assumption, we obtain much smaller estimated parameters than in Cariboni and Schoutens (2009). A careful selection of the initial parameters is needed in the VG-OU case as well.

After some preliminary attempts, as a starting point in the optimization procedure we consider (0.3, 0.025, 0.065, 0.005) for the CIR model, (0.75, 2, 100, 0.005) and (0.5, 0.5, 25, 0.005) for the Gamma-OU and the IG-OU models, (1, 0.5, 100) for the Sato-Gamma model, and (0.75, 20, 250, 400, 0.005) for the VG-OU model.

Figure 2 shows the behavior of the RMSE of the calibrated one-factor models across companies (median, 95th, and 15th percentile are reported) with regularization. The pricing error is high between the end of 2008 and the first half of 2009. At first sight, it might seem that the two optimization approaches provide similar pricing errors and

for this reason we report only the results of the regularized problem. In the following we show only median, mean, 90th, and 10th percentile values and we do not report minimum and maximum values of the variables of interest. We do this to exclude possible outliers that may affect the explanatory power of the results shown in Fig. 2. These outliers are principally due to companies with the highest CDS spreads.

Furthermore, we define a market distress measure (MDM) given by the distance between bid and ask spreads, that is

$$MDM = \sqrt{\sum_{T_i} \frac{\left(c_{T_i}^{CDS\ bid} - c_{T_i}^{CDS\ ask}\right)^2}{4 \cdot \text{number of observations}}}. \tag{17}$$

The number 4 (=2^2) in the denominator comes from the fact that we are considering the semi-difference between bid and ask spreads. For each model and for each company, we count the number of days in which the RMSE exceeds the MDM, that is

$$\text{Exceedances} = \frac{\sum_t I_{\{RMSE_t > MDM_t\}}}{\text{numbers of days}}$$

where t indicates the time component. The 4 in the denominator of Eq. (17) implies that we have a satisfactory pricing performance if the difference between the market price and the model price is not greater than half of the bid-ask spread, or equivalently, the model price is greater than the ask and less than the bid price. This is one possible way to include a market distress component into the pricing exercise. The true price lies somewhere between the bid and ask price, therefore we have a poor calibration if the model price is not on average between these prices. In practice, when the RMSE exceeds the MDM, we have a bad calibration; if not, the model exhibits good performance. As the market becomes less stable, the measure MDM starts to increase, therefore a larger pricing error is allowed.

Figure 3 reports the behavior of MDM, where median, mean, and percentiles are computed across all 117 companies. Furthermore, by considering all the companies analyzed, Fig. 4 shows for all calibrated models the boxplot for the number of days for which an exceedance occurs. The figure shows that the regularization enhances the calibration exercise in the IG-OU and the VG-OU cases. Under the IG distributional assumption, the choice of the starting point and the regularization play a major role. In the regularized optimization approach the VG-OU model is, on average, the best performing and the Sato-Gamma is the worst. In the CIR and the Gamma-OU cases, the pricing error of the model with $\rho = 100$ is slightly greater than the model with $\rho = 0$. Under the Sato assumption, the regularization does not affect the finding of the optimal parameters. In both non-regularized and regularized approaches, the VG-OU model produces slightly smaller errors, at least for the data investigated in this study. This is not surprising since the VG-OU model has the largest number of parameters.

Regarding parameter stability, as outlined by Kokholm and Nicolato (2010), the Sato process, even if with only 2 degrees of freedom, demonstrates more stable parameters as shown in Figs. 5 and 6. As shown in similar empirical studies, we estimate

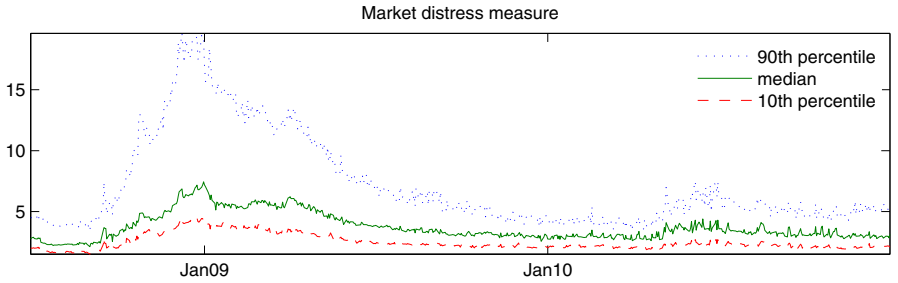

Fig. 3 Behavior of the median, mean, 90th and 10th percentile over 117 companies included in the iTraxx Index of the market distress measure (in bp) from 30 June 2008 to 31 December 2010

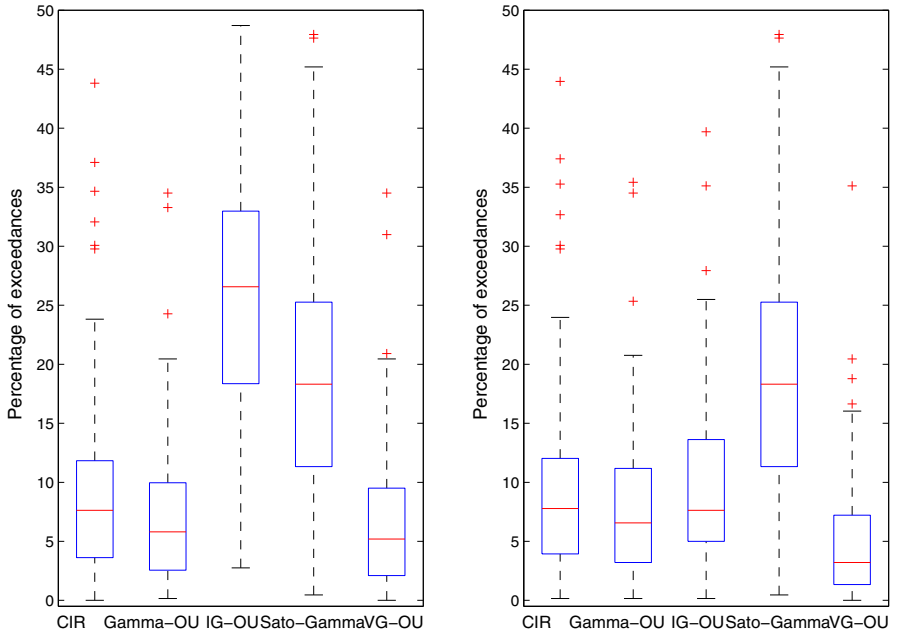

Fig. 4 Percentage of exceedances (across companies) for the CIR, the Gamma-OU, the IG-OU, the Sato-Gamma, and the VG-OU models with regularization term $\rho = 0$ (left side) and with regularization term $\rho = 100$ (right side). On each box, the central mark is the median, the edges of the box are the 25th and 75th percentiles, the whiskers extend to the most extreme data points not considered outliers, and outliers are plotted individually

the autocorrelation of the parameters in order to assess parameter stability over time. Figure 7 shows the average autocorrelation for each model parameter across companies. A value around 0 indicates a very low stability; a value around 1 indicates high stability. As expected, the regularized optimization technique improves parameter stability over time in all the cases considered (see also the Appendix). As far as parameter stability is concerned, the Sato-Gamma model outperforms the four competitor models. Furthermore, the Sato-based model does not show big differences between the regularized and the non-regularized optimization approaches.

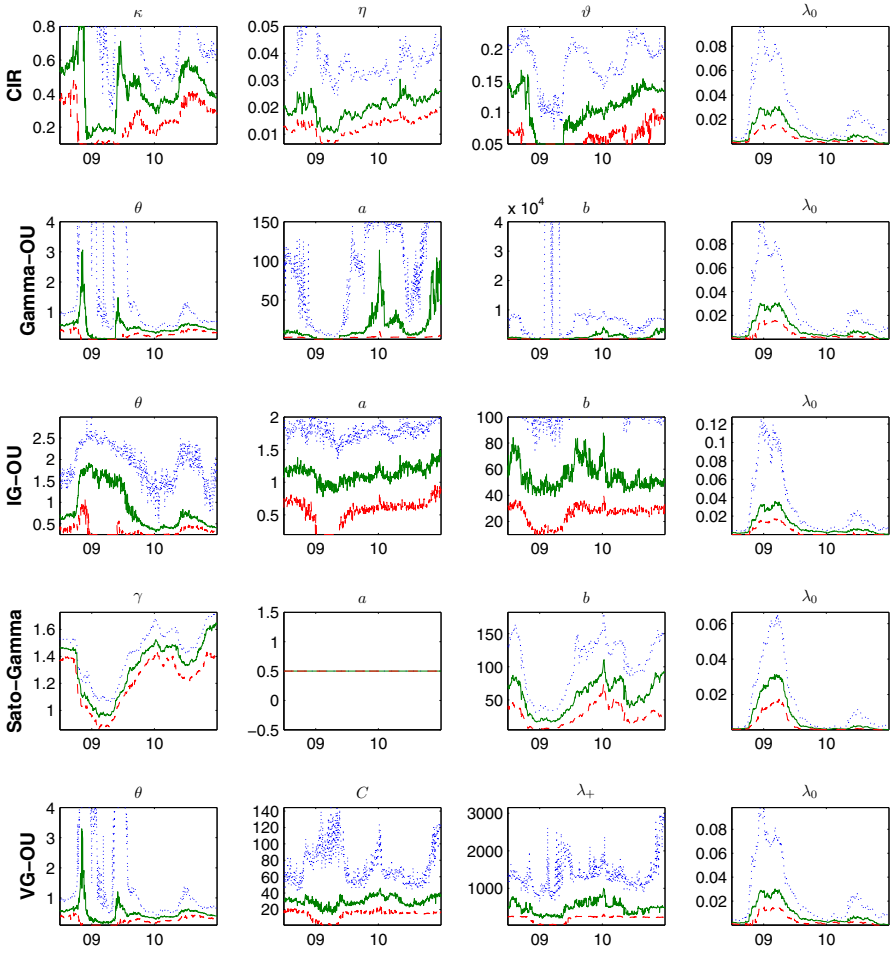

Fig. 5 Parameters median, 90th and 10th percentile for 117 companies included in the iTraxx Index estimated by considering the CIR, the Gamma-OU, the IG-OU, the Sato Gamma, and the VG-OU model from 30 June 2008 to 31 December 2010 without regularization, that is $\rho = 0$. The parameter λ_- of the VG-OU model is not reported

5.2 A Dynamic Perspective: The Long-Term Convergence Trader Approach

In the market maker case the model parameters are calibrated on CDS spreads at each given point in time and these parameters can vary over time. In the long-term convergence trader case the dynamics of CDS spreads are explained by a unique set of parameters that are kept fixed over time. For each company, under the static approach we perform a point-in-time estimation and under the dynamic approach we extract both the unobservable intensity process and the related parameters by the whole term structure of CDS spreads (the so-called *state and parameter estimation*). It is clear that a dynamic consistency is more difficult to achieve than a static consistency, and a more sophisticated calibration method is needed.

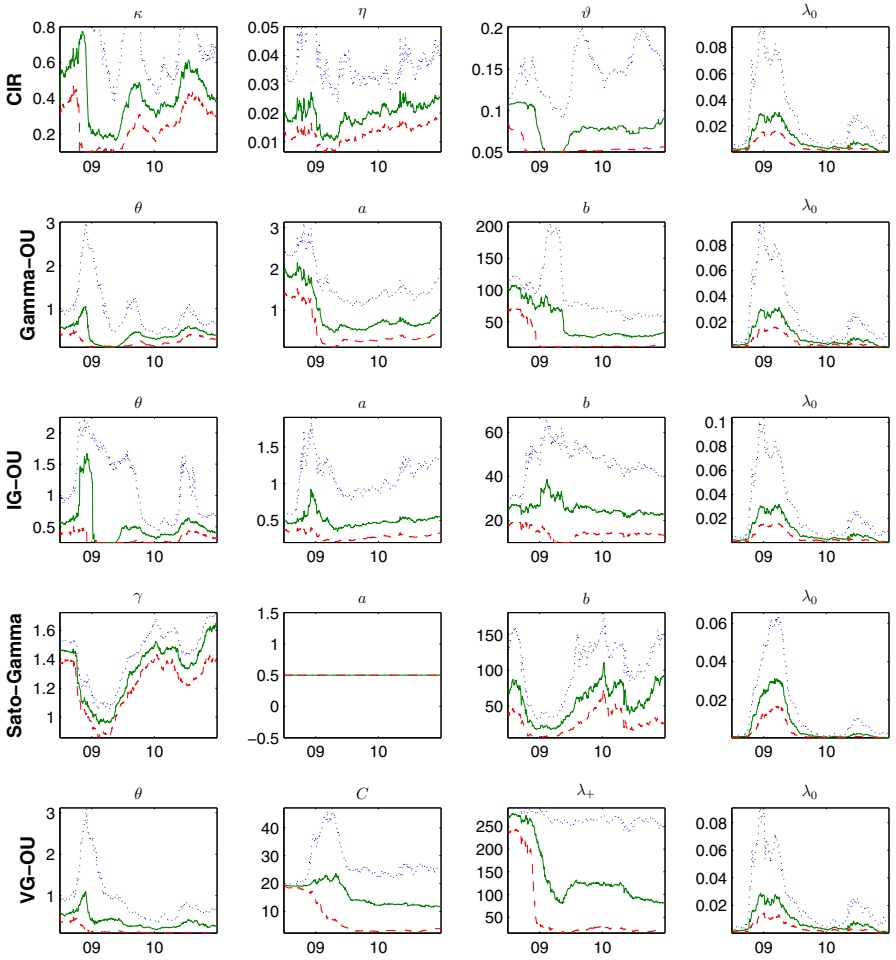

Fig. 6 Parameters median, 90th and 10th percentile for 117 companies included in the iTraxx Index estimated by considering the CIR, the Gamma-OU, the IG-OU, the Sato Gamma, and the VG-OU model from 30 June 2008 to 31 December 2010 with regularization term, that is $\rho = 100$. The parameter λ_- of the VG-OU model is not reported

Filtering methods are standard tools to explore the behavior of the interest rate term structure (see, for example, the works of Brigo and Hanzon 1998 and Duan and Simonato 1999) and they have been successfully applied in a state-space framework to extract the unobservable factors from observed rates. However, there are only a few research papers that cast the default term structure into a state-space form and calibrate it with a filter (see Chen et al. 2008; Jarrow et al. 2011; Carr and Wu 2010 and Chen et al. 2013). Recently, Li (2011) analyzed and explained the use of filtering methods and applied them to option pricing models.

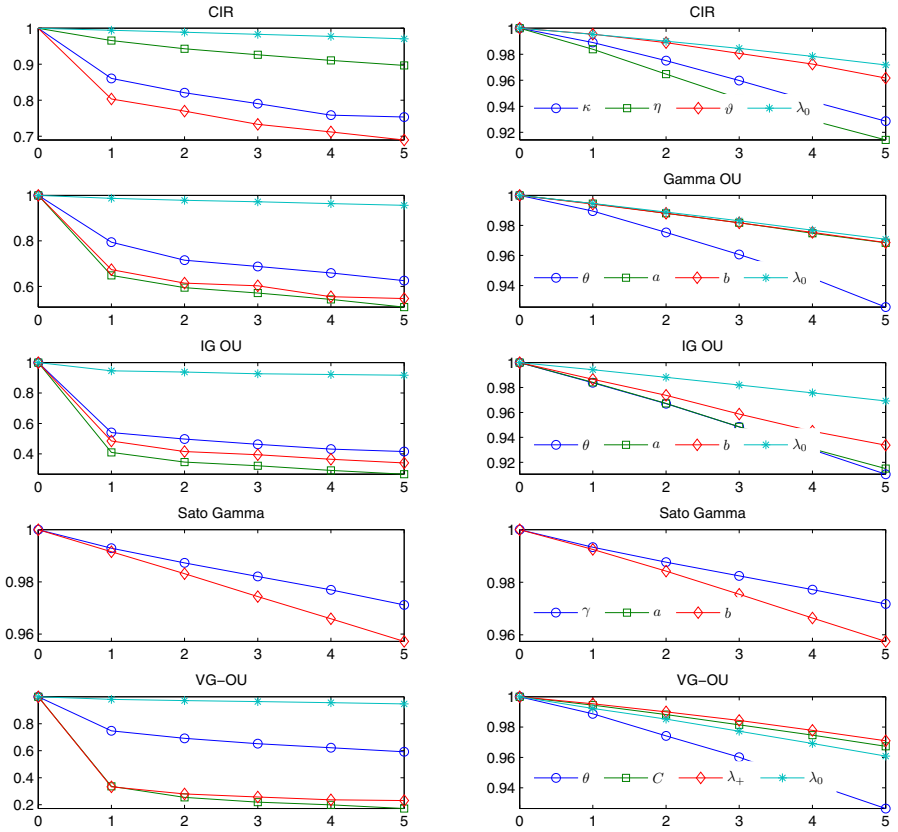

Fig. 7 Autocorrelation as a function of the lag for the CIR, the Gamma-OU, the IG-OU, the Sato-Gamma, and the VG-OU estimated parameters. Average values across companies. On the left, we report the autocorrelations without regularization term into the optimization problem, that is $\rho = 0$, on the right, we report the autocorrelations with regularization term $\rho = 100$ into the optimization problem

In all the cases we are interested in, the model can be written in the following form

$$\begin{aligned} \lambda_t &= f(\lambda_{t-1}, \Theta, v_{t-1}) \\ z_t &= h(\lambda_t, \Theta, \varepsilon_t) \end{aligned} \tag{18}$$

where t is the day counter, λ_t is the state variable (also referred to as the latent or unobservable factor) that can be also a multidimensional variable, and v_{t-1} is the randomness from the state variable. The state variable follows the dynamics described by f. The variable z_t represents the set of observations, in our case the CDS spreads observed in the market. Then, the function h is the so-called measurement function, which in our case is given by the CDS pricing formula, and it depends on the state variable, model parameters, and measurement noise ε_t. A standard hypothesis assumes that this measurement noise is normally distributed: since we consider five CDS spread observations each day, we have a five-dimensional normally distributed error. Even

though the measurement error covariance matrix R can be set as a non-diagonal matrix, it is chosen to be diagonal in this study and therefore the covariance structure of default intensity is represented only by the model itself and not by the measurement error covariance matrix. Furthermore, in order to provide a better estimation error, the measurement error covariance is adjusted for the daily observed bid-ask spreads, that is, the diagonal covariance matrix is multiplied by a diagonal matrix with diagonal entries equal to observed bid-ask spreads.

The state variable in Eq. (18) can be filtered to compute the likelihood function to maximize in order to obtain a state and parameter estimation. By following van der Merwe et al. (2001) and Chen et al. (2013), in the unscented Kalman filter case, and Bhar (2010) and Malik and Pitt (2011), in the particle filter case, and under the assumption of normally distributed errors, it is possible to obtain a quasi-maximum likelihood estimate; that is, one can compute the log-likelihood function LL_t at each time t, and the joint log-likelihood for the entire observed sample is

$$LL(\Theta) = \sum_{t=1}^{T} LL_t. \tag{19}$$

We are assuming that the error component is normal, but the state variable can be any Markov process. For each step, we assume that the measurement errors on each series are independent and identically distributed. The maximum likelihood estimator (MLE) then can be computed by solving the following optimization problem

$$\hat{\Theta} = \max_{\Theta} LL(\Theta). \tag{20}$$

As discussed above, the algorithm provides the simultaneous state and parameter estimation. To resume, the estimation algorithm can be implemented as follows.

Step 1 At time 0, take an initial guess for the set of parameters Θ_0, the state variable λ_0 and for the diagonal matrix R.
Step 2 Estimate the state variable with a filtering method and generate model prices.
Step 3 Compare the model prices with the market ones and evaluate the log-likelihood function in Eq. (19).
Step 4 Insert the log-likelihood evaluation procedure (steps 1 to 3) into an optimization procedure in order to find the solution for problem (20).

Since the model proposed in Eq. (18) is non-Gaussian with respect to the state variable and not linear with respect to the measurement function, the classical Kalman filter cannot be used. The filtering methods considered here are based on the extensions of the Kalman filter, that is the unscented Kalman filter (UKF) and the particle filter, (PF) as described by van der Merwe et al. (2001). Inference with filtering methods has been widely studied, see for example the works of Lopes and Tsay (2011), and applied in finance. Ad-hoc statistical Maltab libraries are available on the web. A slight modification of the code proposed by De Freitas (see http://www.cs.ubc.ca/~nando/) has been used in the empirical study, in both the UKF and the PF cases. In this paper we do not go into detailed explanations of computational issues related to this field:

they have little to do with financial modelling and more to do with statistical and programming problems.

In the rest of this section we analyze under a filtering perspective the same one-factor models already studied in Sect. 5.1. However, we focus only on the CIR and the VG-OU models. By considering that the VG distribution for the case in which $\lambda_+ < \lambda_-$ is asymmetric, the proposed VG-OU process presents positive and negative jumps of different sizes and, at least in theory, it allows a more flexible calibration. However, this greater flexibility comes at the expense of the positivity of simulated trajectories. In order to overcome this theoretical drawback, we use a practical trick (see O'Sullivan 2008). Indeed, in both the CIR and the VG-OU cases, to ensure the factor does not become negative we replace possible negative values of the factor with 10^{-5} (though this occurs rarely). In this part of the paper we do not deal with Sato-based models. By construction, Sato-based models do not present a stochastic default intensity (as stated in Eq. (12) the intensity is deterministic), as they are defined by directly modelling the process A_t in Eq. (1). Then, we exclude also the Gamma and IG based models because, under a dynamic perspective, they do not seem to provide an acceptable level of calibration error in the fitting of observed CDS spreads. The main drawback is the lack of negative jumps in the trajectory that makes a slow return to stability levels after large positive jumps. Cont and Kan (2011) observed that the use of models which allow only upward jumps may not be sufficient to explain the two-sided heavy-tailed behavior of CDS spreads.

5.2.1 Assessing the Filters' Capabilities: A Simulation Study

In this section we propose a simulation study of two different filtering methods, that is the UKF and the PF, in order to assess the estimation methodology. First, intensity processes are simulated and then CDS prices are computed with a certain normal measurement random noise with given covariance matrix $\sigma_\varepsilon I$, where σ_ε is a constant and I is the unit matrix.

The simulation study is performed by assuming two different dynamics for the mean-reverting process driving the default intensity (CIR and VG-OU). As already discussed in Sect. 5.2, the Gamma-OU and the IG-OU are not considered since they show poor performance, mostly attributable to the fact that they allow only for positive jumps. We extract the risk-free rate from the LIBOR swap curve for short-term maturities up to 9 months and the EU swap curve for maturities from 1 year to 30 years from June, 30 2008 to December 31, 2010, for a total of 655 observation days, as described in Sect. 4. We simulate 655 CDS spreads for each model and for each maturity (1, 3, 5, 7, and 10 years). More precisely, we use the following procedure:

Step 1 By considering a one-factor model, we simulate an intensity process with a given parameters set Θ_0.

Step 2 Given the intensity process (the state variable), we compute the corresponding CDS spreads.

Step 3 We simulate the normal measurement noise with zero mean and covariance matrix $\sigma_\varepsilon I$ ($\sigma_\varepsilon = 10$) and then add the noise to the CDS spreads.

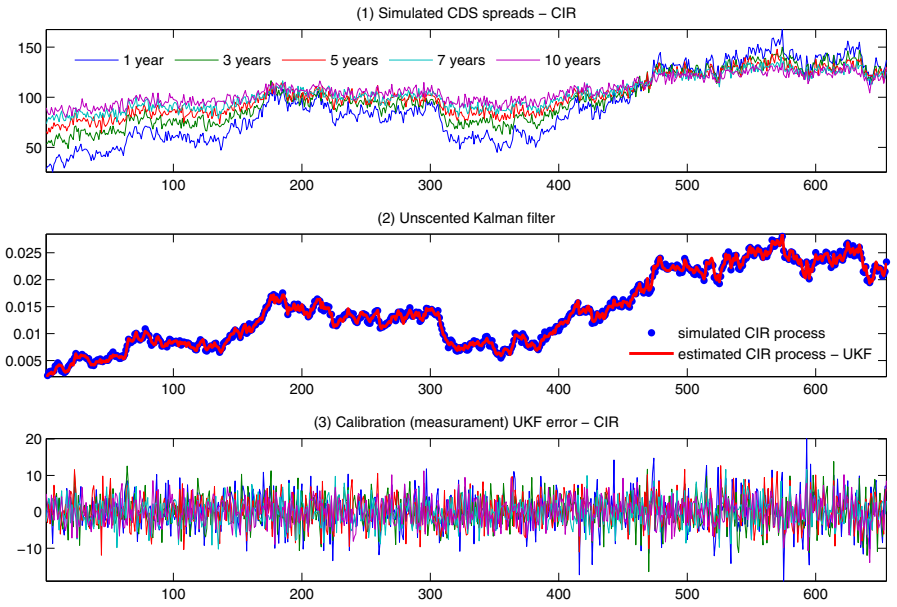

Fig. 8 CIR model: **1** Simulated CDS spreads with normal noise, **2** CIR default intensity process and UKF estimate, **3** UKF calibration error. Risk-free rates are extracted from market data between 30 June 2008 to 31 December 2010. The unscented Kalman filter is considered to extract the unobservable default intensity process

Step 4 For each day, we calibrate the one-factor model by following the method proposed in Sect. 5.1 (for a total of 655 sets of parameters).

Step 5 We compute the median values Θ_{median} of the parameters computed in Step 4 (across all 655 sets of parameters) and only λ_0 is set to be equal to the parameter estimated for the first observation day.

Step 6 By taking as starting point Θ_{median}, we estimate the default intensity process and the parameters with a filtering method.

Step 7 We compare the estimated intensity process with the simulated one.

In the CIR case, we consider the set of parameters $(\kappa, \eta, \vartheta, \lambda_0, \sigma_\varepsilon)$ equal to (0.35, 0.02, 0.1, 0.0025, 10). Figure 8 shows simulated CDS spread data, the simulated CIR process, the estimated unobservable CIR process extracted through the unscented Kalman filter from the simulated CDS spread data, and the pricing errors across different maturities. As shown in Fig. 8, the estimated (and unobservable) default intensity process is close to the simulated one, showing a suitable performance of the estimation methodology.

The CIR model does not allow for jumps in the default intensity, and this implies that it may not be able to capture sharp movements in the market. Conversely, the VG-OU model allows for jumps in the default intensity and, at least in theory, can capture sharp movements in the market and for this reason we also study it. In the VG-OU case, we consider the set of parameters $(\theta, C, \lambda_+, \lambda_-, \lambda_0, \sigma_\varepsilon)$ equal to (0.75, 20, 500, 1,000, 0.0025, 10). Figure 9 shows simulated CDS spread data, the simulated VG-OU

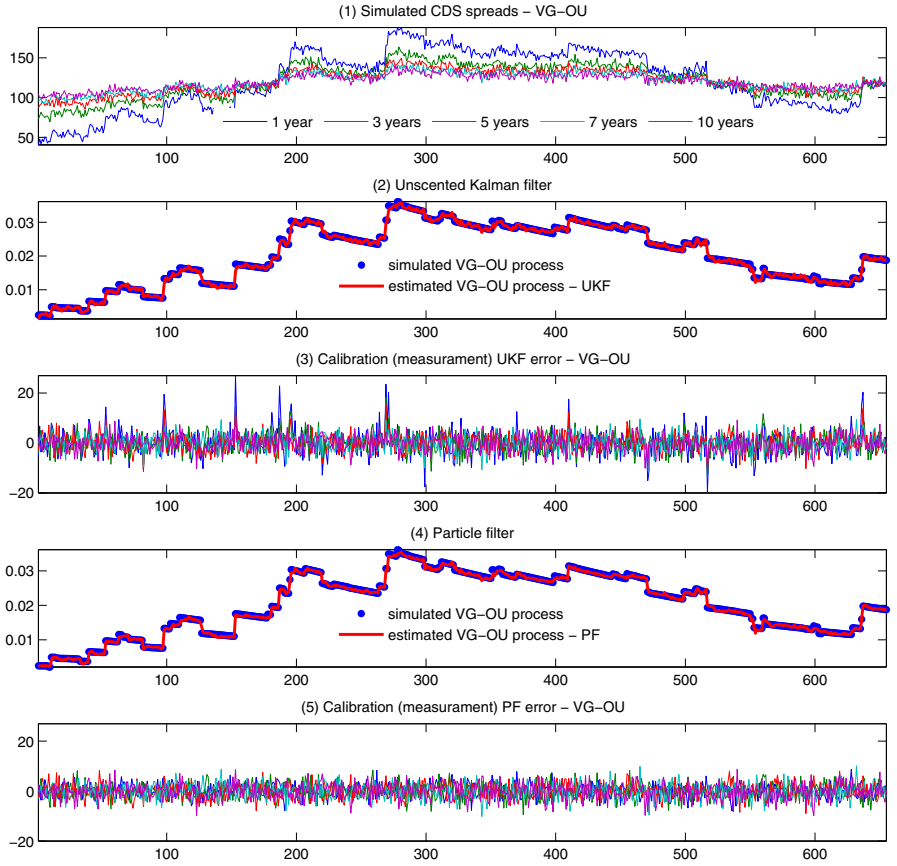

Fig. 9 VG-OU model: **1** Simulated CDS spreads with normal noise, **2** VG-OU default intensity process and UKF estimate, **3** UKF calibration error, **4** VG-OU default intensity process and PF estimate, **5** PF calibration error. Risk-free rates are extracted from market data between 30 June 2008 to 31 December 2010. The unscented Kalman filter and the particle filter are considered to extract the unobservable default intensity process

process, the estimated unobservable VG-OU process extracted through the UKF and the PF from the simulated CDS spread data, and the pricing error across different maturities for both filtering methods. As shown in Fig. 9, the unobservable default intensity process estimated with the PF method has a smaller pricing error, indicating suitable performance of the estimation methodology. The intensity process estimated with the UKF method presents poorer performance than the process estimated with the PF method because it is not able to capture large jumps.

However, as expected, in the UKF case, the optimization procedure converges faster towards a local minimum. As observed by Kantas et al. (2009), in the PF case the maximum likelihood parameter estimation method is more challenging because one has to deal with a likelihood function estimate that is not continuous with respect to Θ and, consequently, the optimization routine shows poor convergence properties. Further-

more, to avoid the degeneration of the particle weights, which leads to a few particles containing most of the probability mass, and to make the sequential simulation-based techniques viable (see Candy 2009 chapter 7), we consider a stratified resampling scheme (see Douc and Cappé 2005 and references therein).

We point out that under the VG-OU assumption the likelihood evaluation procedure in the unscented Kalman filter case is more than 50 times faster than in a particle filter case with 1,500 particle simulations. The computing time increases if one considers more particles or a more complex Lévy-based model. The computational cost of the resampling step is of minor concern with respect to the computational cost of the simulation step and of the evaluation of the measurement function h. The evaluation of the measurement function h accounts for more than 70 % of the computational time and the simulation step for 25 %. We stress that we face the same problem under the CIR assumption and have a similar computational cost. In the particle filter case we simulate 1,500 particles at each time step. Furthermore, in order to reduce the variance and to improve the stability of the algorithm, random variates are kept fixed into the optimization routine. In Lévy-based models, one may have to deal also with memory allocation problems as the number of particles increases. This is of minor concern if one can use the 64-bit version of Matlab on a 64-bit operating system or if the random numbers generator algorithm allows the seed to be set. We run the particle filter estimate on an Opteron platform with Matlab R2011a and, in order to reduce the algorithm variance, we fix six matrices of uniform variates of which the four largest have the dimension $1,500 \times 100 \times 655$ or, alternatively, we set the seed of the generator. If one considers an unscented particle filter algorithm (see van der Merwe et al. 2001), even with a small number of random variates (200 particles), the computational time increases, because most of the time is spent in the computation of the proposal distribution (UKF step).

5.2.2 Estimation on Market Data

In this section we investigate the filtering based estimation on real CDS spread data described in Sect. 4. In Fig. 10 we report the results of the maximum likelihood estimates based on the UKF and the PF method. First, we consider the UKF approach. Recall that the average relative percentage error (ARPE) is defined as

$$ARPE = \frac{1}{\text{number of observations}} \sum_{observations} \frac{|c^{CDS\ market} - c^{CDS\ model}|}{c^{CDS\ market}}.$$

Under this approach both the RMSE and ARPE are smaller in the VG model. The median (mean) ARPE is 10.02 % (10.13 %) in the CIR case and 9.39 % (9.82 %) in the VG case. The computational time, evaluated as the number of function evaluations in the optimization procedure, is larger in the VG case compared to the CIR case (the median is more than 950 against around 500 function evaluations). As already observed in Sect. 5.2, for each company the dynamics of CDS spreads over time are explained by a unique set of parameters. Therefore, the boxplots in Fig. 10 show the variations of these parameters across all 117 companies analyzed. By taking into

consideration the results in Sect. 5.1, in the optimization procedure the parameters (κ, η, ϑ, λ_0) move in the region between (0.1, 0.005, 0.05, 1e-5) and (0.8, 0.05, 0.25, 2.5) in the CIR based model and (θ, C, λ_+, λ_-) move in the region between (0.1, 1, 50, 50) and (4, 100, 750, 1,000) in the VG-OU based model. In both cases the diagonal elements of the diagonal matrix R range between 1 and 100. Note that the parameter C hits the boundary in most cases and the median value is 100 (the mean value is 65.40). By construction, positive jumps are always greater than negative ones, as the marginal distribution VG is assumed to be asymmetric with $\lambda_+ < \lambda_-$. The median difference between λ_- and λ_+ is slightly more than 40 (the mean difference is slightly more than 120). This difference between the positive and the negative tails in the VG based model seems to be the factor that decreases the calibration error with respect to the normal-based model. However, as already proved in Sect. 5.2.1, the UKF approach is not able to properly to assess the benefits arising from the presence of jumps in the dynamics of the default intensity and for this reason we calibrate the model by applying a particle filter approach.

As already observed, in Fig. 10 we also report the results of the maximum likelihood estimates based on the PF method. As the optimization problem's starting point, we consider the UKF estimates. In the PF case too, the estimates do not show remarkable differences. The computational time of the two models, evaluated as the number of function evaluations into the optimization procedure, is similar. The median (mean) ARPE is 9.19 % (9.67 %) in the CIR case and 8.92 % (9.30 %) in the VG case. Note that the parameter C hits the boundary in most cases, and the median value across all 117 companies analyzed is 99.98 (the mean is 79.39). The median difference between λ_- and λ_+ is nearly 43 (the mean difference is nearly 120).

The estimates related to the matrix R show that the calibration error depends on the maturity. In particular, Fig. 10 shows large values for the elements r_{11} and r_{55} of the diagonal matrix R, which correspond to the 1-year and 10-year maturity, respectively. Conversely the element r_{22} corresponding to the 3-year maturity is the smallest in the CIR case (r_{33} in the VG-OU case, respectively). This means that the calibration error is large for the shortest and the longest maturity and, conversely it is small for the 3-year maturity (5-year, respectively). The use of a one-factor model allows us to calibrate only partially the inverted spreads observed during the recent market downturns. The calibration error is large in the mean (nearly 10 %). The present calibration exercise confirm that the proposed one-factor models are not able exactly to calibrate the dynamics of CDS spreads over time. Even if the VG-OU model outperfoms the CIR model under the static setting, it does not show remarkable differences with respect to the Gaussian competitor in the dynamic setting analyzed.

Besides estimating the parameters in both models, we apply the Akaike information criterion (AIC) to identify the superior model. The AIC is evaluated as

$$AIC = 2np - 2LL$$

where np is the number of parameters and LL is the model's log-likelihood. According to the AIC, the VG-OU model (PF estimate) is better because in 110 cases out of 117 its AIC value is less than the AIC value of the CIR model (UKF estimate). In 89 cases out of 117 the AIC of the VG-OU model (PF estimate) is less than the AIC value of

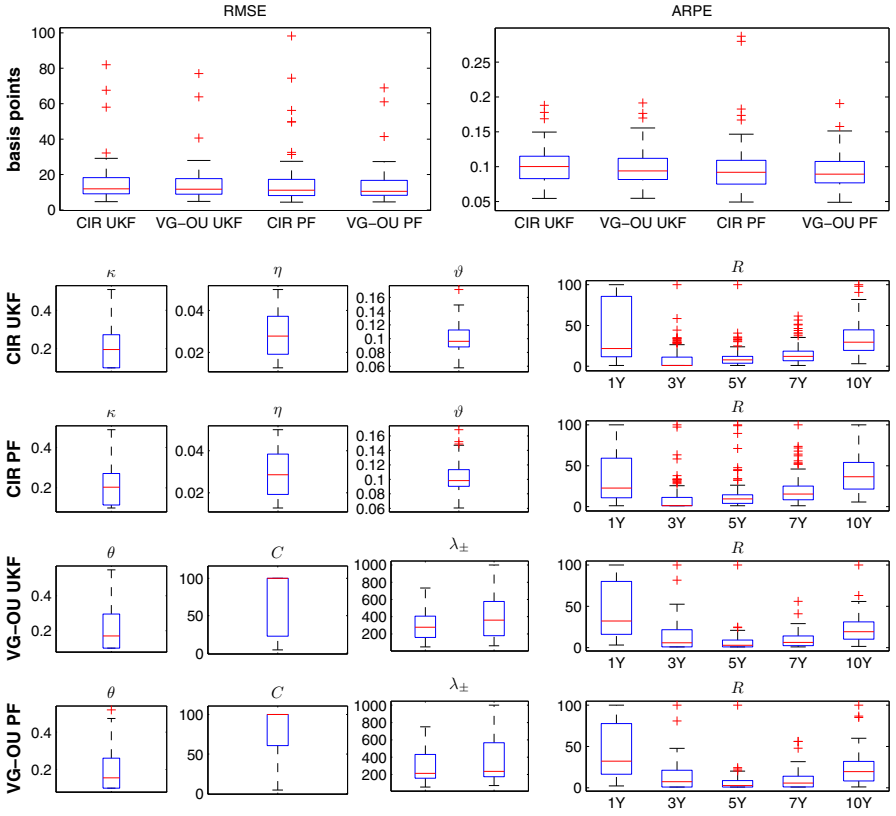

Fig. 10 Maximum likelihood estimates based on the UKF and the PF: RMSE, ARPE and parameters boxplot across all 117 companies analyzed are reported. The estimates of the CIR and the VG-OU are compared by considering both the UKF and the PF approach. On each box, the central mark is the median, the edges of the box are the 25th and 75th percentiles, the whiskers extend to the most extreme data points not considered outliers, and outliers are plotted individually

the CIR model (PF estimate). The AIC shows that the proposed VG-OU model can be useful in explaining sharp movements in the CDS market.

6 Conclusions

In this paper we present an empirical study of CDS no-arbitrage pricing models by following two different estimation methods: (1) we study the models' performance under a static perspective and (2) we analyze the dynamics of the default process over time by considering filtering methods.

In the first empirical analysis, pricing performance, parameter stability and model performance adjusted for general market behavior are measured across different models and across a wide range of companies. It is shown that, although all selected models have a large pricing error during the period of market distress, the RMSE relative to

CIR and OU processes is small, with median values across all companies less than 4 basis points over the entire time window. The Sato assumption does not allow for an effective calibration of observed spreads, even if parameters are quite stable over time. As far as parameter stability is concerned, the CIR parameters have autocorrelations similar to the OU model parameters, and the Sato-Gamma parameters are more stable over time. The parameter stability can be improved by including regularization techniques into the optimization procedure. Furthermore, we note that in some cases the CIR parameters hit the boundary included in the optimization procedure to avoid the intensity process reaching zero. Regarding the models' performance adjusted for general market behavior, and measured as the number of times the model price is between bid and ask prices, both CIR and OU processes show a satisfactory performance for at least 50 % of the companies included in the sample, with less than 15 % exceedances (10 % in the VG-OU case). For the Sato process the number of exceedances is greater.

The dynamic analysis shows that only the CIR and the VG-OU models can effectively be used to calibrate market CDS spreads under a state-space approach. The use of Lévy-based OU processes that allow only for positive jumps (i.e., Gamma-OU and IG-OU) is obstructed by the path properties of these processes, which do not seem suitable to replicate the behavior of observed CDS spreads quoted in the market. The VG-OU process allows for two-sided jumps and it may be used in practical applications. However, this process is driven by a non-Gaussian random variable and therefore the use of more complex filtering method is needed to obtain reliable estimates and to assess the benefits arising from the presence of jumps in the dynamics of the default intensity. Finally, because the mean calibration error is nearly 10 %, we can conclude that the proposed one-factor models are not always able exactly to calibrate the dynamics of CDS spreads over time. The VG-OU model does not show remarkable differences in terms of calibration error with respect to the Gaussian competitor under the dynamic setting analyzed. However, it can be useful to calibrate more volatile CDS spreads to explain sharp variations in CDS spreads. This is confirmed by the fact that, applying the Akaike information criterion, we find empirical evidence that the VG-OU model outperforms the common CIR model.

Acknowledgments Michele Leonardo Bianchi acknowledges that the views expressed in this article are those of this author and do not involve the responsibility of the Bank of Italy.

Appendix

Stability Analysis of the Regularized Optimization Problem

The non-linear least square optimization problem defined in Eq. (16), that is

$$\hat{\Theta} = \min_{\Theta} \left(RMSE(\Theta) \right)^2 \tag{21}$$

has neither a closed-form solution nor a global minimum. A numerical optimization routine is needed to find a relative minimum also because the gradient vector and the Hessian matrix related to the problem are difficult to express in closed-form: even if they can be computed, they have a messy expression. In this paper we follow the practical approach described in Fang et al. (2010); indeed we define the regularized problem

$$\hat{\Theta} = \min_{\Theta} \left(RMSE(\Theta)^2 + \rho \|\omega \cdot (\Theta - \Theta_0)\|^2 \right). \tag{22}$$

where ρ is a constant term and ω is a vector defined to provide a comparable parameter sensitivity as the parameters may differ significantly in magnitude. The vector ω is given by $(1/\Theta_0^1, \ldots, 1/\Theta_0^N)$, where N is the length of Θ and with "$\cdot$" we indicate the inner products of vectors. The choice is aimed at achieving a satisfactory calibration error and parameter stability over time.

In this appendix we study how, by increasing the value of the parameter ρ, the parameters, calibration errors and computational time vary. The selection of a proper ρ is itself an optimization problem which has to be solved to find a solution to the original least squares problem. As already observed in Sect. 5.1, ρ depends on the data at hand and on the level of error present in it. In Table 2 we report the results of the empirical study conducted over time and across all the 117 companies analyzed. More precisely, we show the lag-5 autocorrelation computed by considering the parameter time series of each company. Then we compute median and mean values across all companies. As expected, the parameter stability increases by increasing ρ, even if some parameters are more volatile than others. Additionally, we report median and mean values of the RMSE, of the average relative percentage error (ARPE) and of the number of function evaluations into the optimization routine. The number of function evaluations is a proxy for the computational time. These values are computed both over time and across all the 117 companies analyzed. By increasing the value of ρ, we find that the calibration error increases in the CIR and in the Gamma-OU cases, it remains quite stable in the Sato Gamma case, and in the IG-OU and in the VG-OU cases it reaches the minimum value when ρ=10. The computational time decreases in the CIR case and, conversely, increases in the Sato-Gamma case. The value ρ=100 shows a good balance between the calibration error and the parameter stability and for this reason we selected this value in the main text of the paper. In the empirical study we solve a large number of problems of the form of (22): for each model and across the 117 companies we consider 655 daily observations for a total of more than 380,000 daily calibration exercises. For this reason, even if the selected value of ρ may be not the optimal value, it is sufficient for our purposes as it provides us with an acceptable calibration error and parameter stability. As shown in Table 2, when ρ is equal to 100, the median values for the ARPE are just over 2 per cent (less than 1.5 per cent if we do not consider the Sato based model) and the median lag-5 autocorrelations are all above 0.9. Finally, we note that Table 2 confirms that the VG-OU model outperforms its competitor models while having a comparable degree of parameter stability over time and of computational complexity, not only when ρ is equal to 100, but also for all other selected values of ρ.

Table 2 Lag-5 autocorrelation of the parameters, calibration error and computing time

		ρ						
		0	10	50	100	200	500	1000
CIR	κ	0.7535	0.8427	0.9063	0.9286	0.9471	0.9701	0.9755
		0.7354	*0.8333*	*0.8973*	*0.9217*	*0.9408*	*0.9587*	*0.9676*
	η	0.8969	0.9049	0.9112	0.9141	0.9164	0.9183	0.9187
		0.8789	*0.8902*	*0.8995*	*0.9039*	*0.9068*	*0.9079*	*0.9076*
	ϑ	0.6897	0.9219	0.9491	0.9618	0.9728	0.9789	0.9809
		0.6806	*0.9150*	*0.9392*	*0.9548*	*0.9642*	*0.9690*	*0.9689*
	λ_0	0.9707	0.9712	0.9717	0.9718	0.9720	0.9725	0.9721
		0.9631	*0.9636*	*0.9642*	*0.9646*	*0.9649*	*0.9652*	*0.9653*
	RMSE	1.4025	1.4067	1.4379	1.4985	1.5211	1.5966	1.7498
		2.6759	*2.6950*	*2.7290*	*2.7544*	*2.7902*	*2.8672*	*2.9609*
	ARPE	0.0148	0.0149	0.0150	0.0153	0.0154	0.0161	0.0173
		0.0189	*0.0190*	*0.0194*	*0.0197*	*0.0200*	*0.0209*	*0.0220*
	Function evaluations	173	111	100	99	99	99	100
		179.3526	*127.2661*	*110.7324*	*106.5334*	*103.9400*	*101.7892*	*101.1559*
Gamma-OU	θ	0.6252	0.8018	0.8866	0.9257	0.9516	0.9679	0.9724
		0.5969	*0.7771*	*0.8683*	*0.8999*	*0.9340*	*0.9607*	*0.9696*
	a	0.5094	0.9549	0.9678	0.9684	0.9667	0.9631	0.9563
		0.5034	*0.9470*	*0.9526*	*0.9526*	*0.9530*	*0.9500*	*0.9441*
	b	0.5470	0.9561	0.9659	0.9686	0.9664	0.9661	0.9635
		0.5089	*0.9354*	*0.9543*	*0.9591*	*0.9594*	*0.9615*	*0.9592*
	λ_0	0.9560	0.9671	0.9702	0.9708	0.9711	0.9718	0.9719
		0.9488	*0.9581*	*0.9610*	*0.9623*	*0.9635*	*0.9646*	*0.9651*
	RMSE	1.2899	1.3287	1.3857	1.4165	1.4797	1.6557	1.7717
		2.1841	*2.2086*	*2.2782*	*2.3190*	*2.3748*	*2.4779*	*2.5811*
	ARPE	0.0141	0.0143	0.0147	0.0151	0.0157	0.0164	0.0175
		0.0171	*0.0175*	*0.0182*	*0.0185*	*0.0191*	*0.0202*	*0.0212*
	Function evaluations	161	97	93	90	88	84	83
		183.0975	*100.7687*	*94.8180*	*92.1618*	*89.7360*	*86.7029*	*84.8406*
IG-OU	θ	0.4160	0.8759	0.8887	0.9105	0.9302	0.9586	0.9720
		0.4038	*0.8645*	*0.8848*	*0.9037*	*0.9246*	*0.9494*	*0.9647*
	a	0.2672	0.9185	0.9145	0.9150	0.9276	0.9389	0.9401
		0.2796	*0.9027*	*0.8979*	*0.9035*	*0.9142*	*0.9193*	*0.9288*
	b	0.3409	0.9267	0.9335	0.9338	0.9351	0.9433	0.9480
		0.3494	*0.9054*	*0.9143*	*0.9191*	*0.9264*	*0.9300*	*0.9429*
	λ_0	0.9164	0.9655	0.9682	0.9692	0.9704	0.9715	0.9726
		0.8924	*0.9572*	*0.9602*	*0.9616*	*0.9621*	*0.9642*	*0.9653*

Table 2 continued

		ρ						
		0	10	50	100	200	500	1000
	RMSE	1.9670	1.4611	1.4880	1.4787	1.5127	1.5534	1.6158
		5.8222	*2.8714*	*2.6187*	*2.8030*	*2.6454*	*2.6749*	*2.7028*
	ARPE	0.0196	0.0156	0.0154	0.0157	0.0158	0.0163	0.0172
		0.0391	*0.0199*	*0.0196*	*0.0197*	*0.0200*	*0.0205*	*0.0210*
	Function evaluations	137	96	87	87	87	87	88
		159.1480	*109.2036*	*103.1158*	*101.0573*	*100.2680*	*99.2605*	*97.1306*
Sato-Gamma	γ	0.9712	0.9712	0.9713	0.9718	0.9719	0.9725	0.9728
		0.9667	*0.9668*	*0.9670*	*0.9672*	*0.9674*	*0.9679*	*0.9682*
	b	0.9572	0.9573	0.9574	0.9575	0.9586	0.9608	0.9631
		0.9520	*0.9522*	*0.9526*	*0.9531*	*0.9538*	*0.9556*	*0.9579*
	RMSE	2.1090	2.1090	2.1091	2.1091	2.1091	2.1126	2.1352
		5.0287	*5.0287*	*5.0291*	*5.0299*	*5.0323*	*5.0423*	*5.0634*
	ARPE	0.0219	0.0219	0.0220	0.0219	0.0220	0.0222	0.0226
		0.0270	*0.0271*	*0.0271*	*0.0271*	*0.0272*	*0.0274*	*0.0278*
	Function evaluations	56	36	36	36	36	36	36
		55.4030	*37.0428*	*37.0146*	*36.9764*	*36.8857*	*36.6916*	*36.4880*
VG-OU	θ	0.5920	0.8311	0.8862	0.9264	0.9423	0.9595	0.9646
		0.5780	*0.8032*	*0.8744*	*0.9033*	*0.9273*	*0.9517*	*0.9645*
	C	0.1724	0.9465	0.9676	0.9674	0.9721	0.9735	0.9778
		0.2059	*0.9330*	*0.9562*	*0.9550*	*0.9645*	*0.9604*	*0.9600*
	λ_-	0.2801	0.9607	0.9669	0.9692	0.9734	0.9757	0.9783
		0.2950	*0.9580*	*0.9544*	*0.9510*	*0.9526*	*0.9538*	*0.9582*
	λ_+	0.2308	0.9556	0.9658	0.9710	0.9753	0.9799	0.9822
		0.2581	*0.9501*	*0.9573*	*0.9628*	*0.9698*	*0.9731*	*0.9727*
	λ_0	0.9468	0.9389	0.9544	0.9609	0.9664	0.9698	0.9707
		0.9399	*0.9188*	*0.9397*	*0.9484*	*0.9547*	*0.9616*	*0.9633*
	RMSE	1.2255	1.0152	1.0656	1.1284	1.1969	1.3060	1.4217
		2.0193	*1.5918*	*1.7065*	*1.7950*	*1.8805*	*2.0379*	*2.1731*
	ARPE	0.0134	0.0103	0.0114	0.0120	0.0126	0.0141	0.0149
		0.0163	*0.0140*	*0.0150*	*0.0157*	*0.0163*	*0.0176*	*0.0187*
	Function evaluations	188	145	129	127	123	116	112
		258.2815	*162.6107*	*140.6695*	*133.6337*	*127.1655*	*118.6974*	*113.1985*

For each model and for each parameter median and mean values (in italics) of the lag-5 autocorrelation are computed over the 117 companies analyzed. Then, median and mean (in italics) values of the root mean square error (RMSE), of the the average relative percentage error (ARPE) and of the number of function evaluations into the optimization routine are computed both over time and over the 117 companies analyzed

References

Amadei, L., Di Rocco, S., Gentile, M., Grasso, R., & Siciliano, G. (2011). Credit default swaps: Contract characteristics and interrelations with the bond market. Discussion Papers: Consob, n. 1.

Barndorff-Nielsen, O. E. (1997). Processes of normal inverse Gaussian type. *Finance and Stochastics*, *2*(1), 41–68.

Barndorff-Nielsen, O. E., & Shephard, N. (2001). Non-Gaussian Ornstein–Uhlenbeck based models and some of their uses in financial economics. *Journal of the Royal Statistical Society: Series B (Statistical Methodology)*, *63*(2), 167–241.

Bhar, R. (2010). *Stochastic filtering with applications in finance*. Singapore: World Scientific.

Bianchi, M. L., Rachev, S. T., & Fabozzi, F. J. (2013). Tempered stable Ornstein-Uhlenbeck processes: A practical view. Working Paper, Bank of Italy, n. 912.

Bibby, B. M., & Sørensen, M. (2003). Hyperbolic processes in finance. In S. T. Rachev (Ed.), *Handbook of heavy tailed distributions in finance* (pp. 211–248). Amsterdam: Elsevier.

Brigo, D., & El-Bachir, N. (2010). An exact formula for default swaptions pricing in the SSRJD stochastic intensity model. *Mathematical Finance*, *20*(3), 365–382.

Brigo, D., & Hanzon, B. (1998). On some filtering problems arising in mathematical finance. *Insurance: Mathematics and Economics*, *22*(1), 53–64.

Brigo, D., & Mercurio, F. (2006). *Interest rate models—Theory and practice: With smile, inflation, and credit*. Berlin: Springer.

Candy, J. V. (2009). *Bayesian signal processing: Classical, modern, and particle filtering methods*. New York: Wiley.

Cariboni, J., & Schoutens, W. (2009). Jumps in intensity models: investigating the performance of Ornstein-Uhlenbeck processes in credit risk modeling. *Metrika*, *69*(2), 173–198.

Carr, P., & Wu, L. (2010). Stock options and credit default swaps: A joint framework for valuation and estimation. *Journal of Financial Econometrics*, *8*(4), 409–449.

Carr, P., Geman, H., Madan, D., & Yor, M. (2007). Self-decomposability and option pricing. *Mathematical Finance*, *17*(1), 31–57.

Chen, R. R., Cheng, X., Fabozzi, F. J., & Liu, B. (2008). An explicit, multi-factor credit default swap pricing model with correlated factors. *Journal of Financial and Quantitative Analysis*, *43*(1), 123–160.

Chen, R. R., Cheng, X., & Wu, L. (2013). Dynamic interactions between interest-rate and credit risk: Theory and evidence on the credit default swap term structure. *Review of Finance*, *17*(1), 403–441.

Cont, R. (2001). Empirical properties of asset returns: Stylized facts and statistical issues. *Quantitative Finance*, *1*(2), 223–236.

Cont, R. (2010). Credit default swaps and financial stability. In *Financial Stability Review* (Vol. 14, pp. 35–43). Paris: Banque de France.

Cont, R., & Kan, Y. (2011). Statistical modeling of credit default swap portfolios. Working Paper.

Cont, R., & Tankov, P. (2004). *Financial modelling with jump processes*. Boca Raton: CRC Press.

Cox, J. C., Ingersoll, J. E., & Ross, S. A. (1985). A theory of the term structure of interest rates. *Econometrica*, *35*(2), 385–408.

Douc, R., & Cappé, O. (2005). Comparison of resampling schemes for particle filtering. In *Proceedings of the 4th International Symposium on Image and Signal Processing and Analysis* (pp. 64–69). IEEE.

Duan, J. C., & Simonato, J. G. (1999). Estimating and testing exponential affine term structure models by Kalman filter. *Review of Quantitative Finance and Accounting*, *13*(2), 111–135.

Duffie, D., & Garleanu, N. (2001). Risk and valuation of collateralized debt obligations. *Financial Analysts Journal*, *57*(1), 41–59.

Duffie, D., & Singleton, K. J. (1999). Modeling term structures of defaultable bonds. *Review of Financial Studies*, *12*(4), 687–720.

Duffie, D., Filipović, D., & Schachermayer, W. (2003). Affine processes and applications in finance. *Annals of Applied Probability*, *13*(3), 984–1053.

Dunbar, K. (2008). US corporate default swap valuation: the market liquidity hypothesis and autonomous credit risk. *Quantitative Finance*, *8*(3), 321–334.

Fang, F., Jönsson, H., Oosterlee, K., & Schoutens, W. (2010). Fast valuation and calibration of credit default swaps under Lévy dynamics. *Journal of Computational Finance*, *14*(2), 57–86.

Hull, J., Predescu, M., & White, A. (2004). The relationship between credit default swap spreads, bond yields, and credit rating announcements. *Journal of Banking and Finance*, *28*(11), 2789–2811.

Jarrow, R. A., Li, H., & Ye, X. (2011). Exploring statistical arbitrage opportunities in the term structure of CDS spreads. Working Paper, National University of Singapore.

Kantas, N., Doucet, A., Singh, S. S., & Maciejowski, J. M. (2009). An overview of sequential Monte Carlo methods for parameter estimation in general state-space models. In *Proceedings of the 15th IFAC Symposium on System Identification (SYSID)*. Saint-Malo, France.

Kokholm, T., & Nicolato, E. (2010). Sato processes in default modelling. *Applied Mathematical Finance*, *17*(5), 377–397.

Lando, D. (2004). *Credit risk modeling: Theory and applications*. Princeton: Princeton University Press.

Li, J. (2011). Sequential Bayesian analysis of time-changed infinite activity derivatives pricing models. *Journal of Business and Economic Statistics*, *29*(4), 468–480.

Lopes, H. F., & Tsay, R. S. (2011). Particle filters and Bayesian inference in financial econometrics. *Journal of Forecasting*, *30*(1), 168–209.

Malik, S., & Pitt, M. K. (2011). Modelling stochastic volatility with leverage and jumps: A simulated maximum likelihood approach via particle filtering. Working Paper, Banque de France, n. 318.

Mandelbrot, B. (1963). The variation of certain speculative prices. *Journal of Business*, *36*(4), 394–419.

Mayordomo, S., Peña, J. I., & Schwartz, E. S. (2013). Are all credit default swap databases equal? *European Financial Management*.

O'Kane, D., & Turnbull, S. (2003). *Valuation of credit default swaps*. Lehman Brothers: Fixed Income Quantitative Credit Research.

O'Sullivan, C. (2008). Parameter uncertainty in Kalman-Filter estimation of the CIR term structure model. In J. A. D. Appleby, D. C. Edelman, & J. H. Miller (Eds.), *Numerical methods for finance*. London: Chapman & Hall.

Pan, J., & Singleton, K. J. (2008). Default and recovery implicit in the term structure of sovereign CDS spreads. *Journal of Finance*, *63*(5), 2345–2384.

Rachev, S. T., & Mittnik, S. (2000). *Stable Paretian models in finance*. New York: Wiley.

Rachev, S. T., Kim, Y. S., Bianchi, M. L., & Fabozzi, F. J. (2011). *Financial models with Lévy processes and volatility clustering*. Hoboken: Wiley.

Rebonato, R., McKay, K., & White, R. (2010). *The SABR/LIBOR market model: Pricing, calibration and hedging for complex interest rate derivatives*. Wiley.

Rosiński, J., & Sinclair, J. L. (2010). Generalized tempered stable processes. In *Stability in Probability*. Banach Center Publications.

Sato, K. I. (1991). Self-similar processes with independent increments. *Probability Theory and Related Fields*, *89*(3), 285–300.

Sato, K. I. (1999). *Lévy processes and infinitely divisible distributions*. Cambridge: Cambridge University Press.

Schoutens, W. (2003). *Lévy processes in finance*. West Sussex: Wiley.

Schoutens, W., & Cariboni, J. (2009). *Lévy processes in credit risk*. Hoboken: Wiley.

van der Merwe, R., Doucet, A., De Freitas, N., & Wan, E. (2001). *he unscented particle filter. Advances in neural information processing systems*. Cambridge: MIT Press.

Zhang, S., & Zhang, X. (2008). Exact simulation of IG-OU processes. *Methodology and Computing in Applied Probability*, *10*(3), 337–355.

Reproduced with permission of the copyright owner. Further reproduction prohibited without permission.